**Published by Nigerian Society of Physical Sciences. Hosted by FLAYOO Publishing House LTD**

Proceedings of the Nigerian Society of Physical Sciences

**Journal Homepage: https://flayoophl.com/journals/index.php/pnspsc**

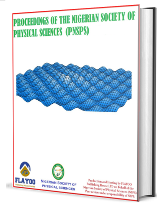

# Investigating the connectivity of Geshere and Rishiwa younger granite using aero-radiometric data

Y. A. Bello[a,*], K. M. Lawal[b], S. S. Magaji[c], J. Raimi[d], T. O. Amuda[a], D. Daramola[a], M. B. Yakubu[d], H. A. Lawal[a]

[a]*Physics Department, Air Force Institute of Technology, Kaduna*
[b]*Physics Department, National Open University of Nigeria, Abuja*
[c]*Geology Department, Ahmadu Bello University, Zaria*
[d]*Physics Department, Ahmadu Bello University, Zaria*

## ABSTRACT

Geshere and Rishiwa Younger Granites (YGs) are physically two separate bodies and are believed to be either from the same source or one is an extension of the other. Previous work suggests they could be connected at the subsurface, but the use of radiometric data can provide clarity as it reflects rocks' geochemical formation. This work focused on identifying possible connection between the two YGs based on the variation of the radioelements in the study area. The result shows the values of potassium, thorium, and uranium range from 0.1 to 4.9 %, 11.9 to 61.2 ppm, and 1.4 to 10.3 ppm respectively, which are lower to the range of the radioelements (that of potassium is comparatively close) reported in part of Egypt. The average potassium concentration around Geshere and Rishiwa is high (4.5 and 4.1 % respectively), thorium is low (13.1 and 14.9 ppm respectively), and uranium is low around Geshere and south of Rishiwa YGs, but high at north of Rishiwa YG. The composite maps of the three radioelements and the potassium reveal the extent of the YGs. The Th/K map indicates the two YGs are connected. Moreover, the composite maps of thorium, and uranium suggested the south of Rishiwa and Geshere share similar geochemistry. Geochemical analysis is recommended on rock samples of a region west of the Gehere YG which is a Pan-Africa Basement Complex but shows anomalies similar to the YGs.

*Keywords:* Geshere, Rishiwa, Radiometric data, Younger granite.

DOI:10.61298/pnspsc.2025.2.151



## 1. INTRODUCTION

The Younger Granites Complexes, YGC, are the primary source of tin mineralization [1]. For instance, the inner area of Ririwai hills has been considerably altered as a result of anthropogenic influences due to the surface and underground tin mining. There are nearly fifty-two younger granite, YG, massifs (including Rishiwa and Geshere YGs) varying in size, and occurred as an extension of the North-South trend of igneous activities which started during the Precambrian at Hoggar in Algeria [1, 2], typically are the ring complexes (Figure 1). YGs are, in addition to tin, associated with cassiterite, zircon, columbite, monazite, tantalite. Thus, stimulating the interest of several geophysical researches.

The YGC of northern Nigeria was described, based on the gravity anomaly over them, as either eupolas or plugs originating

*Corresponding Author Tel. No.: +234-802-2632-598.
*e-mail:* belloya@afit.edu.ng (Y. A. Bello)

from a common, subjacent source batholith or independent intrusions formed in the same way in similar local environments but not physically connected at depth [3]. In the same study, the 3D gravity model indicated the Younger Granite magma originated in the crust by some process of localized selective melting. YGs of the northern Nigeria are characterized by a high-value analytic signal (AS) anomaly from the aeromagnetic data of the area, as compared to the low AS anomaly observed over their host (the Pan-African Basement Complex). The Younger Granites show low Source Parameter Imaging (SPI) depth values of about 4 km below the sea level indicating deeper magnetic sources [1].

The dominant linear structures identified within the YGC of the northern Nigeria through the Center for Exploration Technique (CET) grid analysis of the aeromagnetic data are those trending in NE, NNE and ENE directions with lengths ranging 500 m – 17500 m [4]. These trends were also reported in several works, although extracted trough other techniques [1, 5–7]. The linear structures extracted from aeromagnetic data within the YGC were implied to be weak zones which probably allowed the volcanic eruption that initiated the emplacement of the source of the anomaly [8].

Magnetic anomaly with a signature similar to those associated with ring complexes in part of the YG province but without surface-manifestation are described as unexposed ring complexes having Euler depth solution of about 1800 m [1, 8]. The nature of the unexposed ring complexes (URCs) was attributed to partial subsidence of the enclosed block on which the extrusive edifice of the central volcano originally rested probably occasioned by excess space (much subsurface accommodation) for continuously rising magma within the country rock [1]. A URC was studied in greater details and its lateral dimensions with that of the adjoining ring complexes were better resolved. The URC was found to have a surface area extent of approximately 169.5 km$^2$ which is similar to that of Ririwai, Banke, Kudaru, and Zuku which is 180 km$^2$, 128 km$^2$, 174 km$^2$ and 121 km$^2$, respectively [1]. Its geometry is supportive of aforementioned assertion as it revealed majorly outward dipping trend with depth. Ibeneme *et al*. [1] also attributed the URC to be as a result of incomplete fluidization along the already formed ring fracture and poor assimilation of the country rock by the fluidizing agent amidst a slow/near quiescent piece meal stopping process during the central granite intrusion phase which usually marks the end of ring complex formation.

Geshere and Rishiwa YGs are two complexes that could be thought of as a single complex due to their proximity as can be observed in Figures 1 and 2 [9]. The Euler solution of the aeromagnetic data by Ref. [9] revealed a possible connection of the two YGs at the subsurface. However, there is a need to further verify this finding using other geophysical methods. Ref. [10] reported the radioactive age determination of the YGs provided the most reliable (late Precambrian to early Paleozoic age) suggesting the importance of the application of aero-radiometric data. Moreover, results of radiometric method are usually related to the geology [9, 11–13]. Variations in radiation concentration of potassium (K), thorium (Th) and uranium (U) are related to the presence of lithologies with different chemical and mineralogical composition [14].

This research utilized the aero-radiometric data to map the two YGs to investigate the connectivity between them. Visualizing the variation of the concentrations of the three radioelements, the ratio of potassium (K) with respect to thorium (Th) and uranium (U), and ternary maps provided further insights into the aforementioned claim about the YGs.

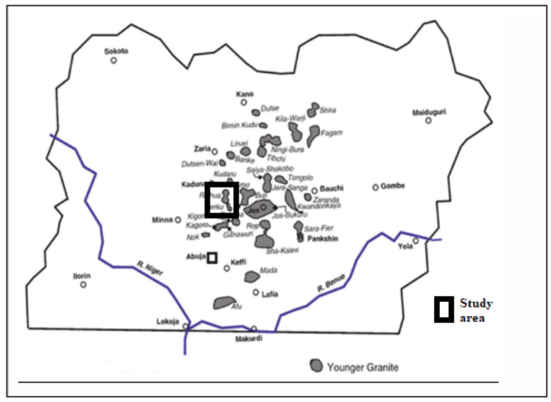


**Figure 1. Map of the study area (Adapted from Ref. [1]).**

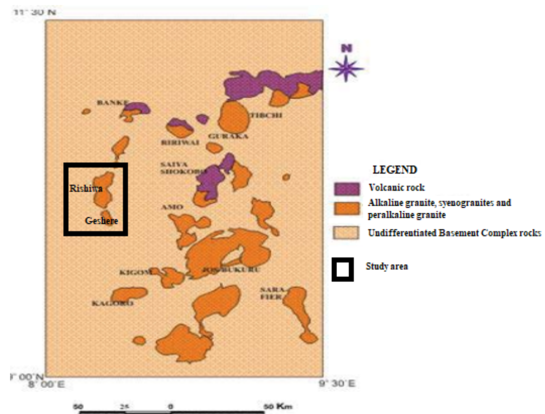


**Figure 2. Geology map of the study area [1].**

### *1.1. GEOLOGY OF THE STUDY AREA*

A detailed geology of the study area has been reported by Ref. [15]. The origin and formation of the Younger Granite ring complexes in Nigeria and beyond were not related to any orogeny and thus are often referred to as being anorogenic in nature. The Younger Granites appear to have been subject to two distinct processes of differentiation resulting in divergent trends viz: a normal series and an alkaline series [15, 16]. The Younger Granites exhibit a large variety of rock types which remain remarkably constant throughout the whole province are Rhyolites, Hornblende-fayalite granites and porphyries, Hornblende-biotite granites, Biotite granites, Riebeckite and Riebeckite-biotite granites, Aegirine arfvedsonite granites, Syenites and Trachytes and Basic rocks (Gabbros, dolerites, basalts etc). Details of occurrence, character and petrography of the rock associations are discussed in Ref. [16]. Some of the Younger Granite ring complexes within the study area are Rishiwa and Geshere (Figure 2).

## 2. MATERIAL AND METHODS

### 2.1. MATERIAL

The aero-radiometric data covering longitude 8 – 8.5° E and latitude 10 – 10.5° N was the primary data used in this study. Aero-radiometric data usually reflect the geology of the study area [17] and the extent of the data used provides the regional information on the variation of the radioelements over the YGs and the Pan-African Basement Complex. The data was obtained from the Nigerian Geological Survey Agency (NGSA).

The data was a part of the airborne survey by Fugro Airborne Survey carried out between 2005 and 2009 on behalf of the Nigerian Geological Survey Agency. The data were acquired along NW – SE flight lines at 500 m line spacing, altitude of 100m, 20 km tie lines spacing and at 80 m terrain clearance. The index sheet covers an estimated area of about 3,025 kilometer-square. The maps are on a scale of 1:100,000 and half-degree sheets [18].

Gamma energy is measured by on-board sodium iodide scintillation counters, GPS position data is stored in the digital data stream. Depending on the speed of the airplane, channels for the overall gamma count, U, Th, and K are individually accumulated, often at one-second intervals that equate to 30 to 60 meters across the ground. Maps displaying the total count and specific radioisotope concentrations (equivalents for U and Th) are produced after the data are corrected for flight height, air temperature, humidity, cosmic noise, Compton scattering, and radon effects. Surficial variables including variations in lithology, soil type, wetness, vegetation, standing water, overburden thickness, terrain, and cultural impacts will almost definitely have an impact on the final data [19].

The data were corrected for background radiation resulting from cosmic rays and aircraft contamination, variations caused by changes in aircraft altitude relative to ground and Compton scattered gamma rays in potassium and uranium energy windows. The uranium and thorium concentrations are, therefore, expressed as equivalent concentrations, eU and eTh, in ppm. Potassium ($^{40}$K) is processed to produce equivalent ground concentrations in %K. Total counts are here converted into (µRhr) called unit of radiation (Ur). The corrected data provide an estimate of the apparent surface concentrations of potassium, uranium and thorium (K, eU and eTh), as well as the total count (TC) values [13].

### 2.2. METHODS

The methods adopted to map the possible extent of the Geshere and Rishiwa Younger Granites are:

i. The TC map, a set of radioelements (K, eU and eTh) contour maps, in addition to their ratios eU/eTh and eU/K) to show the surface distribution of these elements.

ii Establishment of the four composite image maps: radioelement composite image map (K, eU and eTh), equivalent uranium composite image map (eU, eU/eTh and eU/K), equivalent thorium composite image map (eTh, eTh/eU and eTh/K) and potassium composite image map (K, K/eU and K/eTh).

## 3. RESULT AND DISCUSSION

The terrain map (Figure 3) reflects the two Younger Granites having the highest topography in the study area and also indicates the surface area of the Younger granite making it a useful tool to identify effect of the various techniques on the radiometric data of the study area. The YGCs are separated by a river which reflects as a depression in Figure 3. It can be observed that the elevation of the YGs could have contributed to formation and/or sustaining the river that is between them. The total count map (Figure 4) shows the high total count concentration value, 3010.6 Ur, is observed over the peralkaline younger granites and some Pan-African Basement complex. The result also suggests the southern region of the Rishiwa YGC has similar lithological units with the Geshere YGC. Magaji *et al.* [15] classified the lower part of Geshere to be dominant of biotite granite; middle part to be of syenite and arfvedsonite granite; upper part to be more of syenite to arfvedsonite granite. These classifications were reflected in the total count concentration around Geshere YG (Figure 4).

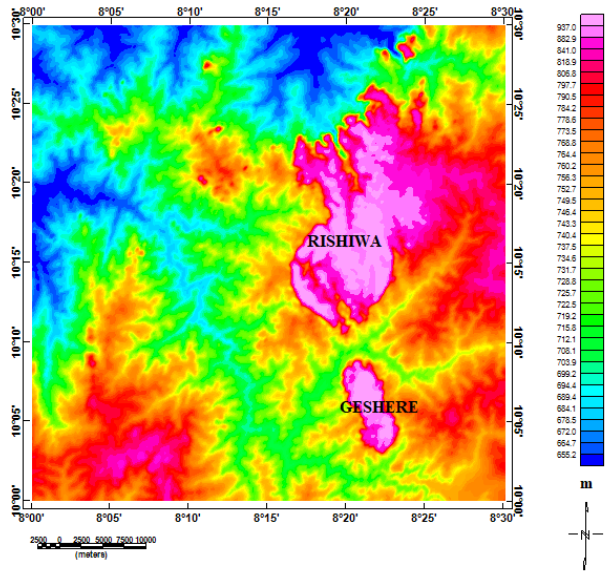


**Figure 3. Digital elevation map of the study area.**

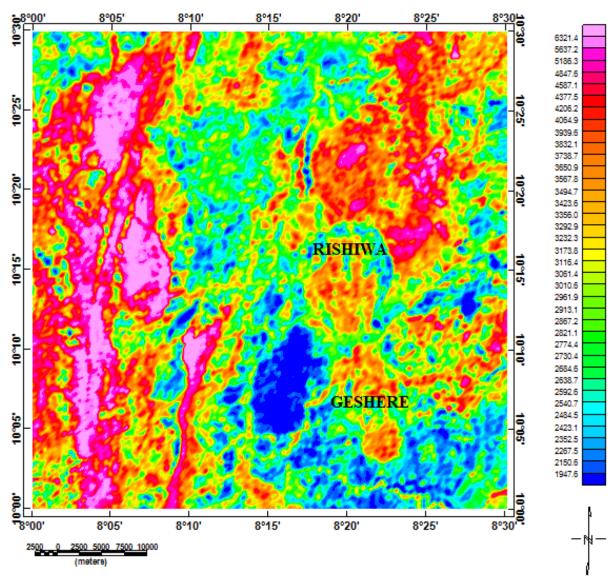


**Figure 4. Total count map of the study area measured (Ur).**

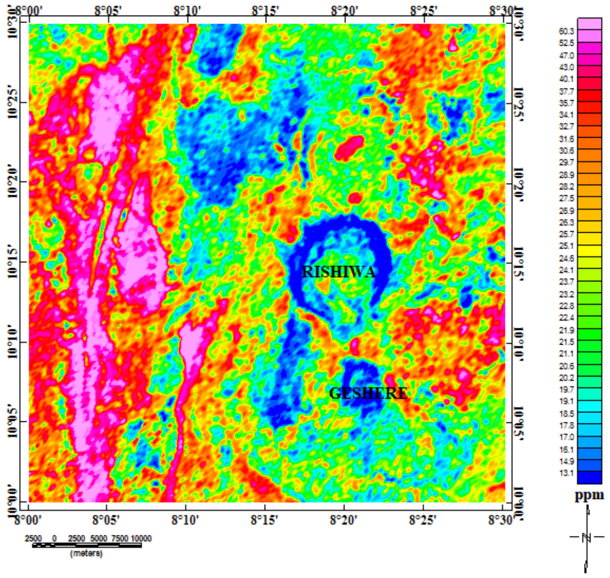


**Figure 5. Thorium map of the study area.**

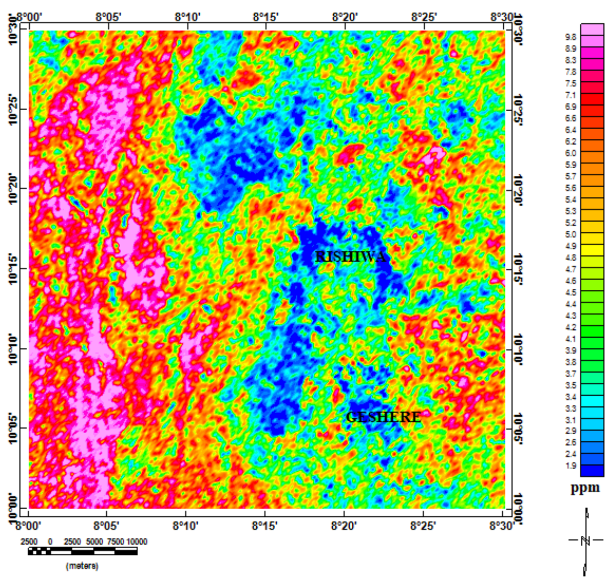


**Figure 6. Uranium map of the study area.**

The maps of eTh map and eU Figures 5 and 6, respectively, show that the southern part of Rishiwa and the northern part of Geshere peralkaline YGs with some Pan-African Basement complexes have the lowest values <18.5 ppm and <3.3 ppm respectively. This is contrary to the report of Ref. [13] on some YGs in Egypt.

Regions of high concentration of Potassium counts are indicative of the migration of Potassium (suggesting possible hydrothermally altered zones) since Potassium is more geochemically active than other radioelements [20]. The K map (Figure 7) shows the overall spatial distribution of the relative potassium concentrations in the study area. It thus indicates that Peralkaline YGs and a region west of the Geshere YG represent the high level (>3.5%) which is in agreement with to the report of Ref. [13]. However, visual inspection of Figures 1, 2, 3, and 7 revealed the region with high potassium concentration, west of the Geshere YG is a Pan-African Basement complex with similar elevation to the YGs. Geochemical analysis of rock sample around the region could shed more light on the geological formation of the region.

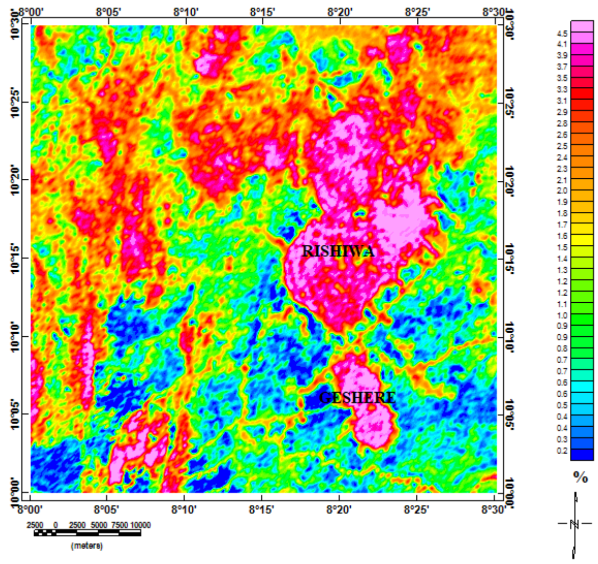


**Figure 7. Potassium map of the study area.**

Careful examination of the K/eTh ratio map (Figure 8) shows that, the highest value (0.178) is recorded over younger granites and the region in the Pan-African Basement complex. Moreover, the dimension of the anomalies agrees with that of the DEM map (Figure 3). In the same vein, the younger granites and the region in the Pan-African Basement complex are associated with highest value of the K/eU (Figure 9). Thorium is commonly considered very immobile [21], thus the areas with low eTh concentration suggests that it was mobilized in hydrothermally altered systems since Thorium depletion is associated with hydrothermal alteration [17]. The ratio maps eTh/K and eU/K (Figures 10 and 11) reveals low values. Figure 11 was made bigger with an arrow showing the gap between the between the YGs is also characterized with low value of the ratio suggesting semblance of connection between the two YGs at the region. Moreover, the Euler solutions in Ref. [9] revealed no contact (i.e. no indication of a body separating the two YGs) solution at that region.

Ternary maps are colour composite images generated by modulating the red, green and blue in proportion to the radioelement concentration values of the K, eTh, eU and their ratio grids. Since particular rock types often have characteristic ratios of the three radioactive elements, the ternary maps of these ratios are a useful geological and mineral exploration tool for discriminating the zones of consistent lithology and contacts between contrasting lithologies [22]. Four composite colour image maps were prepared as follows:

(1) K, eU and eTh (three radioelement composite image map, Figure 12).

(2) K, K/eU and K/eTh (potassium composite image map, Figure 13).

(3) eTh, eTh/eU and eTh/K (equivalent thorium composite im-

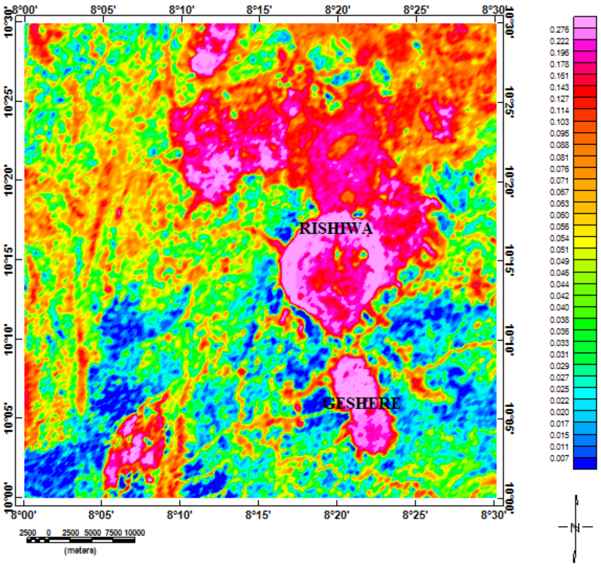


**Figure 8. The ratio map of K and Th of the study area.**

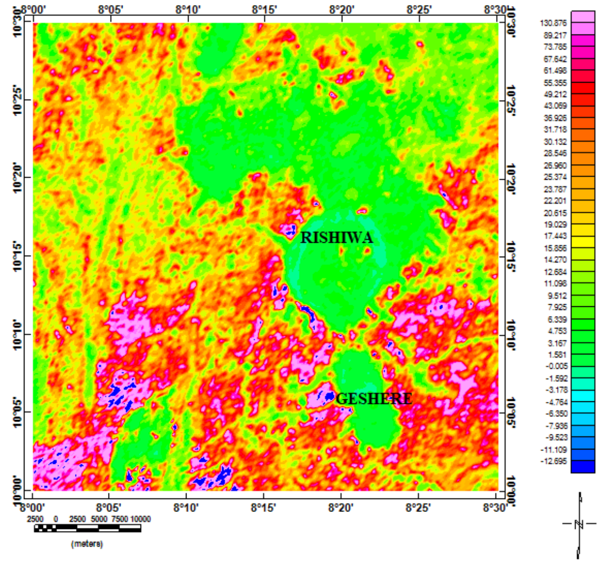


**Figure 10. The ratio map of Th and K of the study area.**

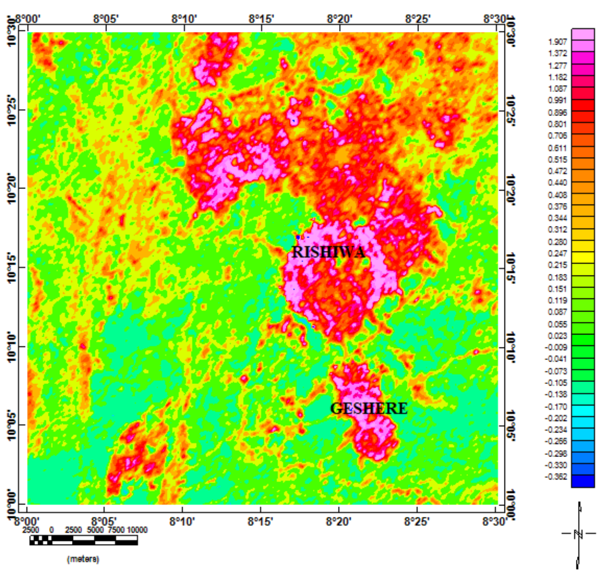


**Figure 9. The ratio map of K and U of the study area.**

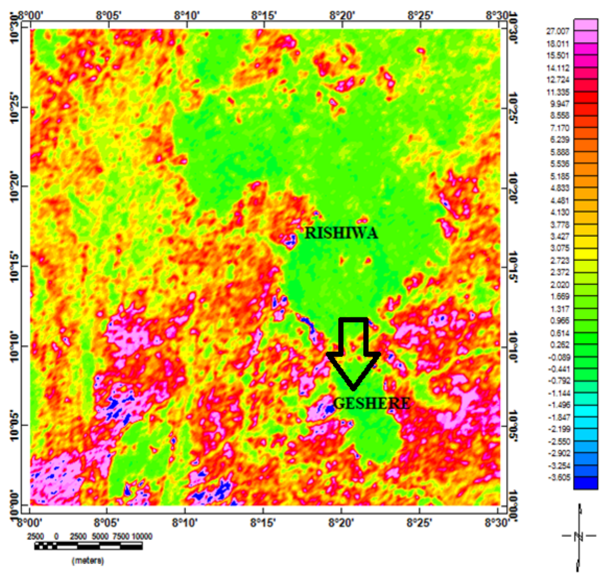


**Figure 11. The ratio map of U and K of the study area.**

age map, Figure 14).

(4) eU, eU/eTh and eU/K (equivalent uranium composite image map, Figure 15).

The three-radioelement composite image map (Figure 12) is produced by using different ink colours to represent the K (in per cent), eU (in ppm) and eTh (in ppm) concentrations. At any location, the relative concentrations of the three radioelements are represented by the colour hue produced by mixing appropriate amounts of the three ink colours [23, 24]. Since a distinct colour hue is used to represent each ternary ratio on the map, zones with similar ratios will be represented by a unique colour. This distinct relationship between colour hue and ternary ratio allows the map to display surface radioelement distribution. Accordingly, different ratios of the three radioelements are displayed as RGB colour combinations. However, younger granites which are normally characterized by their strong radio-spectrometric responses and elemental differences, giving rise to characteristic radioelement ratios [13], are clearly visible on the ternary radioelements map characterized by high concentration of potassium (Figure 12), bright red. High intensity of potassium is an indication of alteration.

The potassium (K) composite image map (Figure 13) combines K (in red) with K/eTh (in green) and K/eU (in blue). This image shows the overall spatial distribution of relative potassium concentrations. The potassium composite image map revealed the two YGs are characterized by high intensity (white colour) of the three components that make up the map. Similarly, the thorium and uranium composite image maps (Figures 14 and 15) revealed equal blend of the three components. The relative con-

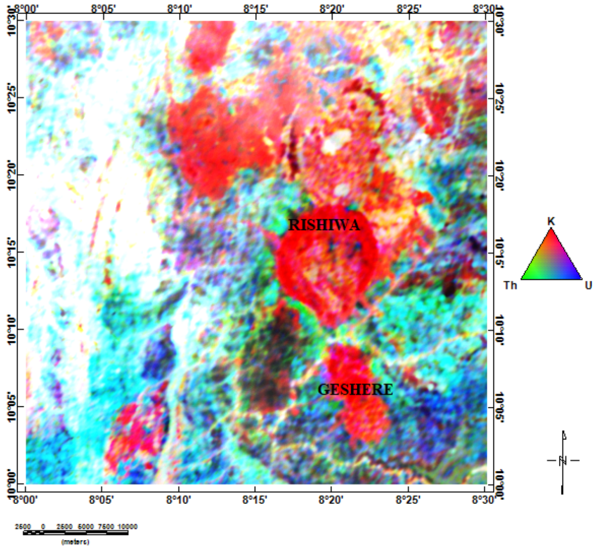


Figure 12. Three radioelement composite image map.

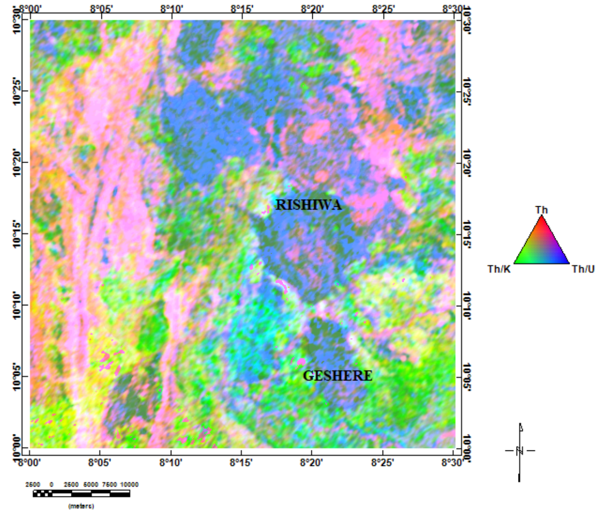


Figure 14. Thorium composite image map.

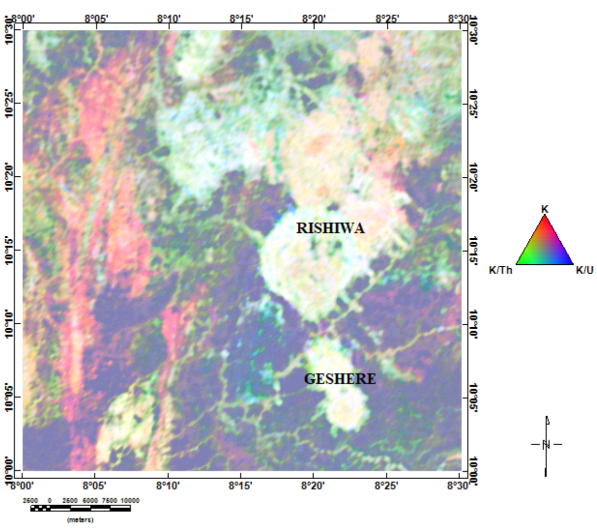


Figure 13. Potassium composite image map.

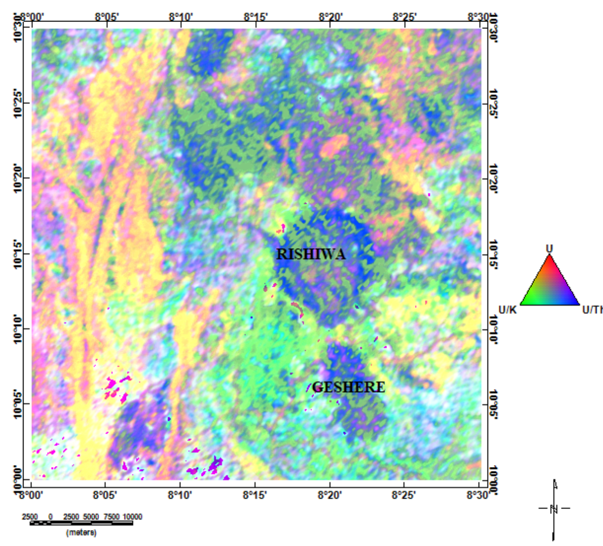


Figure 15. Uranium composite image map.

centrations of eU with respect to both K and eTh is important diagnostic factors in the recognition of possible uranium deposits [25]. This image map also reflects lithological differences and could be useful in geological mapping problems [26].

These anomalous zones are well correlated with the younger granites. These data can distinguish between different types of rock units because of differences in their chemical and physical properties. The river channel, trending NE, a physical feature between the YGs share similar anomaly to the two YGs. The anomaly actually extends from Rishiwa through the river to the Geshere YG signaling they are connected (see Figs. 9 and 10). Some results show evidence of possible similar composition in the southern part of Rishiwa and Geshere and also northern part of Rishiwa and the Pan-African Basement complex west of Geshere (see Figures 4, 9, 12, 13, 14 & 15).

## 4. CONCLUSION

In this research, similar anomaly observed over the YGs and the physical gap between them suggest the two YGs share similar chemical properties. Moreover, some anomaly indicates that the southern part of Rishiwa share much similar chemical properties with Geshere. Therefore, the gap between the two YGs and the identified parts of the YGs will require Geochemical analysis for further verification. The region, west of Geshere YG, a Pan-African Basement Complex, which shows indication of Younger Granite would also require Geochemical analysis of rock samples in the region.

## DATA AVAILABILITY

The data will be available on request from the corresponding author.

## References


[1] S. I. Ibeneme, I. A. Oha , N. N. Abdulsalam & O. K. Mosto, "Improved mapping of the structural disposition of some younger granite ring complexes of Nigeria using high resolution aeromagnetic data," Journal of Geology & Geophysics **7** (2018) 1. https://dx.doi.org/10.4172/2381-8719.1000443.

[2] P. Bowden & J.A. Kinnaird, "Geology and mineralization of the Nigerian anorogenic ring complexes: with a geological map at the scale of 1:500,000", Geologisches Jahrb (Hannover) B **56** (1984) 3. https://www.schweizerbart.de/publication/detail/artno/186025600/Geology_and_mineralization_of_the_Nigerian_anorogenic_ring_complexes.

[3] D. E. Ajakaiye, "Gravity measurements over the nigeria younger granite province", Nature **225** (1970) 50. https://www.nature.com/articles/225050b0.

[4] O. O. Osinowo, K. Alumona & A. I. Olayinka, "Analyses of high resolution aeromagnetic data for structural and porphyry mineral deposit mapping of the nigerian younger granite ring complexes, North - Central Nigeria", Journal of African Earth Sciences **162** (2020) 103705. https://doi.org/10.1016/j.jafrearsci.2019.103705.

[5] C. O. Ofoegbu & K. Hein, "Analysis of magnetic data over part of the younger granite province of Nigeria", PAGEOPH **136** (1991) 173. https://link.springer.com/article/10.1007/BF00876370.

[6] S. Mustapha, S. Suleman, S. R. Iliyasu, E. E. Udensi, Y. A. Sanusi, D. Dahuwa & L. Abba, "Interpretation of aeromagnetic data and landsat imagery over the nigerian younger granites in and around kafanchan area, North-Central Nigeria", FUDMA Journal of Sciences **4** (2021) 323. https://doi.org/10.33003/fjs-2020-0404-489.

[7] A. I. Opara, T. T. Emberga, H. N., Echetama, I. E. Ugwuegbu, K. C., Nwokocha, K. C. Ijeoma, J. C. Chinaka, J. C. Onyema, "Structural interpretation of the jos-bukuru younger granite ring complexes inferred from Landsat-TM data", Journal of Geosciences and Geomatics **3** (2015) 56. https://doi.org/10.12691/jgg-3-3-2.

[8] J. Raimi, B. B. M. Dewu & P. Sule, "An interpretation of structures from the aeromagnetic field over a region in the Nigerian younger granite province", International Journal of Geosciences **05** (2014) 313. https://doi.org/10.4236/ijg.2014.53031.

[9] Y. A. Bello & K. M. Lawal, "Interpretation of aeromagnetic data over the Geshere and Rishiwa Ring Complexes of North-Western Nigeria", Asian Journal of Multidisciplinary Studies **3** (2015) 1. https://www.ajms.co.in.

[10] R. R. E. Jacobson, W. N. McLeod & R. Black, "Ring-complexes in the younger granite province of northern Nigeria", Geological Society of London, Memoir **1** (1958) 5. https://www.lyellcollection.org/doi/pdf/10.1144/gsl.mem.1958.001.01.01.

[11] O. Ademila, A. S. Akingboye & A. I. Ojanomi, "Radiometric survey in geological mapping of basement complex area of parts of Southwestern Nigeria", Vietnam Journal of Earth Sciences **40** (2018) 288. https://doi.org/10.15625/0866-7187/40/3/12619.

[12] H. Syaeful, R. C. Ciputra, T. B. Adimedha, A. Sumaryanto, I. G. Sukadana, F. D. Indrastomo, F. Pratiwi, S. Sucipta, H. A. Pratama, D. Mustika, K. S. Widana, S. Widodo, M. Burhannudinnur, I. Syafri & B. Sutopo, "Radiometric signatures of gold mineralization zone in Pongkor, West Java, Indonesia: a baseline for radiometric mapping application on low-sulfidation epithermal deposit", Resources **13** (2023) 2. https://doi.org/10.3390/resources13010002.

[13] M. A. S. Youssef & S. T. Elkhodary, "Utilization of airborne gamma ray spectrometric data for geological mapping, radioactive mineral exploration and environmental monitoring of southeastern Aswan city, South Eastern Desert, Egypt", Geophys. J. Int., **195** (2013) 1689. https://doi.org/10.1093/gji/ggt375.

[14] T. F. P. de Quadros, J. C. Koppe, A. J. Strieder & J. F. C. L. Costa, "Gamma-ray data processing and integration for lode-Au deposits exploration", Natural Resources Research **12** (2003) 57. https://doi.org/10.1023/A:1022608505873.

[15] S. S. Magaji, R. F. Martin, C. C. Ike & A. E. Ikpokonte, "The Geshere syenite-peralkaline granite pluton: a key to understanding the anorogenic Nigerian younger granites and analogues elsewhere." Periodico di Mineralogia **80** (2011) 199. https://doi.org/10.2451/2011PM0016.

[16] W. N. MacLeod, D. C. Turner & E. P. Wright, "The geology of the Jos Plateau", General Geol Survey Niger Bull **1** (1965) 118. https://catalogue.nla.gov.au/catalog/216693.

[17] A. A. Akinlalu, "Radiometric mapping for the identification of hydrothermally altered zones related to gold mineralization in Ife–Ilesa Schist Belt, Southwestern Nigeria", Indonesian Journal of Earth Sciences **3** (2023) A519. https://doi.org/10.52562/injoes.2023.519.

[18] T. Adewumi, K. A. Salako, U. D. Alhassan, A. A. Adetona, R. A. Abdulwaheed & E. E. Udensi, "Interpretation of Airborne Radiometric data for possible hydrocarbon presence over Bornu basin and its environs, Northeast Nigeria using Thorium normalisation method". Iranian J. of Earth Sci. **13** (2021) 161–172. https://doi.org/10.30495/ijes.2021.682863.

[19] S. Walker, K. Harmen & D. Donovan, "Airborne gamma-ray surveying in hydrocarbon exploration", GeoConvention, Canada, 2018. [Online]. https://geoconvention.com/wp-content/uploads/abstracts/2018/244_GC2018_Airborne_Gamma_Ray_Surveying_in_Hydrocarbon_Exploration.pdf.

[20] S. O. Sanusi & J. O. Amigun, "Structural and hydrothermal alteration mapping related to orogenic gold mineralization in part of Kushaka schist belt, North-central Nigeria, using airborne magnetic and gamma-ray spectrometry data", SN Appl Sci **2** (2020) 1591. https://doi.org/10.1007/s42452-020-03435-1.

[21] A. M. Silva, A. C. B. Pires, A. Mccafferty, R. A. V. de Moraes & H. Xia, "Application of airborne geophysical data to mineral exploration in the uneven exposed terrains of the Rio Das Velhas greenstone belt", Brazilian Journal of Geology **33** (2003) 17. https://ppegeo.igc.usp.br/portal/wp-content/uploads/tainacan-items/15906/45048/9837-11496-1-SM.pdf.

[22] J. S. Duval, "Composite colour images of aerial gamma-ray spectrometry data", Geophysics **48** (1983) 722. https://library.seg.org/doi/pdf/10.1190/1.1441502.

[23] IAEA, "Guidelines for radioelement mapping using gamma-ray spectrometry data", IAEA-TECDOC-1363, Vienna, Austria, 2003, p. 179. [Online]. https://www-pub.iaea.org/MTCD/Publications/PDF/te_1363_web.pdf.

[24] H. J. Broome, "Generation and interpretation of geophysical images with examples from the Rae Provinces, Northwestern Canada Shield ", Geophysics **55** (1990) 977. https://doi.org/10.1190/1.1442927.

[25] IAEA, "Geochemical exploration for uranium", Technical Reports Series, No. 284, IAEA, Vienna, Austria, 1988, p. 96. [Online]. https://www.iaea.org/publications/1387/geochemical-exploration-for-uranium.

[26] B. L. Dickson & K. M. Scoot, "Interpretation of aerial gamma-ray surveys-adding the geochemical factors", AGSO J. Aust. Geol. Geophys. **17** (1997) 187. https://inis.iaea.org/records/66097-qcf39.